

High-field cyclotron resonance and valence-band structure in semiconducting diamond

J. Kono,* S. Takeyama,† T. Takamasu, and N. Miura

Institute for Solid State Physics, University of Tokyo, Roppongi, Minato-ku, Tokyo 106, Japan

N. Fujimori, Y. Nishibayashi, T. Nakajima, and K. Tsuji

Sumitomo Electric Industries Ltd., Koyakita, Itami, Hyogo 664, Japan

(Received 3 May 1993)

The cyclotron resonance of thermally excited free holes has been observed in synthetic semiconducting diamond at ultrahigh magnetic fields up to 150 T generated by the single-turn-coil technique with pulsed far-infrared laser radiations of 28, 36, and 119 μm . Three absorption peaks were observed at and above room temperature for the magnetic fields parallel to the $\langle 100 \rangle$, $\langle 111 \rangle$, and $\langle 110 \rangle$ crystallographic directions. The typical value of $\omega_c \tau$ was as small as 2 at 40°C even in ultrahigh fields. One of the three peaks was observed in the cyclotron-resonance inactive circular polarization for holes, while the other two lines were observed in cyclotron-resonance active circular polarization for holes. Assuming that these resonance absorption lines are due to three holes of the valence bands at the Γ point, i.e., light-hole, heavy-hole, and split-off-hole, we can conclude that the band dispersion curve for one of the three bands has a negative (electronlike) curvature in some directions.

I. INTRODUCTION

Since its discovery by Custers in 1952,¹ type-IIb diamond has been viewed as the prototype covalent semiconductor together with germanium (Ge) and silicon (Si), while at the same time it is a material which will in the future be used for high-temperature semiconductor devices. Although a large number of investigations have been undertaken in order to understand its optical and electrical properties, the understanding is much less profound than that of Ge and Si. Very basic aspects such as the values of carrier effective masses or detailed band structure have been still undetermined. The primary reason for this has been the low carrier mobility as well as the difficulty in growing high-quality single crystals.

As is well known, type-IIb diamond² is a *p*-type extrinsic semiconductor, containing boron as the dominant acceptor; boron is also responsible for the characteristic blue coloration. The activation energy for electrical conduction is approximately 0.35 eV.^{3–6} In the range 100–300°C the dominant carrier scattering process is the acoustical-phonon scattering, in which the temperature dependence of the mobility of holes obeys the $T^{-3/2}$ law.⁴ It is also well known that diamond is an indirect-gap semiconductor with a large indirect energy gap of 5.5 eV. The location of the conduction-band bottom is estimated to be $(\sim \frac{3}{4}, 0, 0)2\pi/a$.^{6,7} The available experimental data on the conduction band are sparse because of the absence of *n*-type semiconducting diamond. The top of the valence band is located at the zone center (the Γ point) just as in Si, Ge, and many III-V compounds. The spin-orbit splitting in the valence band is very small [5–7 meV (Refs. 6 and 8)] compared to that of Ge (290 meV) and Si (44 meV), and this enables the split-off-hole to carry electrical charges in addition to the light and the heavy holes.

Concerning the valence-band parameters, a few works, both experimental and theoretical, have been reported,

but there have been considerable disagreements among authors. The first experimental data are the cyclotron resonance measurements of optically excited holes in natural type-IIb diamond at 70 GHz, and at liquid-helium temperatures reported by Rauch many years ago.^{9,10} The author observed three absorption peaks with little or no anisotropy, and concluded that two bands, the light-hole and heavy-hole bands, are degenerate at $k=0$ with effective masses of $0.70m_0$ and $2.12m_0$, and a third band is split off by 6 meV with a mass of $1.06m_0$. Since this work there have been no reports on the cyclotron resonance in diamond in spite of the great deal of advances in the far-infrared high-field cyclotron resonance technique during the last 30 years.

The average effective mass from Faraday rotation measurements by Prosser is $0.88m_0$,¹¹ and the average from Hall-effect measurements ranges from $0.25m_0$ to $1.1m_0$.^{2,4–6,12} Bagguley *et al.*¹³ studied the Zeeman effect of the acceptor states in type-IIb diamond and obtained the values of the Dresselhaus parameters L , M , and N (Ref. 14) for diamond. Lawaetz¹⁵ calculated the Luttinger parameters in 20 semiconductors, including diamond, by using a five-level $\mathbf{k}\cdot\mathbf{p}$ analysis. Reggiani and co-workers^{16–18} investigated drift mobility and high-field drift velocity in natural diamond with the time-of-flight technique, and obtained density-of-states masses of $0.3m_0$ and $1.1m_0$ for the light hole and heavy hole, respectively. These authors asserted that the masses of Rauch are systematically larger than their experiments, while those of Lawaetz' parameters are systematically smaller. They also reported the electron effective masses $m_e^* = 0.36m_0$ and $m_e^* = 1.4m_0$.¹⁷ There have also been several reports on the determination of Luttinger parameters by the studies of excited states of the acceptor.^{19–21} All the values of the band parameters for diamond reported to date are listed in Table I, where they are converted to the γ parameters (the Luttinger parameters) if they were ex-

TABLE I. The valence-band parameters in diamond reported so far. They are converted to γ parameters (the Luttinger parameters) if they were expressed in other forms in the original papers. Note the considerable discrepancies among authors.

	Lawaetz (Ref. 15) (1971)	Eremets (Ref. 21) (1991)	Bashenov (Ref. 19) (1981)	Bagguley (Ref. 13) (1966)	Rauch (Ref. 10) (1962)
γ_1	4.62	4.24	2.19	2.16	0.94
γ_2	-0.38	0.82	-0.12	-0.23	0.22
γ_3	1.00	1.71	0.87	-0.15	0.25
κ	-0.63				
Method	theory		impurity transitions		CR

pressed in other forms in the original papers.

During the last decade, considerable advances have been made in the technique of ultrahigh-field cyclotron resonance in semiconductors using the destructive single-turn coil method.^{22,23} Many technical difficulties have been overcome, and reliable data have been obtained reproducibly in the magagauss (> 100 T) range.²⁴ This progress has provided us with a powerful tool for investigating the band structures of low-mobility materials which have been previously considered unsuitable for cyclotron-resonance studies and whose properties are not yet well enough understood.²⁵ Many large-gap, heavy-mass semiconductors such as diamond,²⁵ SiC,^{25,26} AlAs,^{25,27} BN, GaN, AlN, etc. fall into this category. In this paper, we present the results of cyclotron resonance of thermally excited carriers in synthetic semiconducting(type-IIb) diamond, which have become possible by virtue of the use of ultrahigh magnetic fields. We also report the results of magnetotransmission experiments on diamond in the millimeter range at fields up to 20 T.

II. EXPERIMENT

Three single-crystal samples 1–3 of semiconducting diamond were studied in pulsed high magnetic fields. They were synthesized at high pressure and high temperature at Sumitomo Electric Industries, Ltd. Sample 1 had the shape of a cubic: two of the six faces were (100) planes, while the other four faces were (110). Each of the faces had an area of about 2.5×2.5 mm². Both samples 2 and 3 had two parallel (111) surfaces with about 1.5-mm thickness. The measurements have been attempted also on several chemical vapor deposition (CVD) type-IIb diamond films deposited on synthetic, bulk single-crystal diamonds, but none of them has yet been successful due to much lower carrier mobility (~ 20 cm²/V s at room temperature) of the films.

Pulsed megagauss magnetic fields used in the present work were produced by the single-turn coil technique.^{22,23,27} The magnetic fields are generated by discharging short, large current pulses of about 2.5 MA to a thin, single-turn copper coil from a fast capacitor bank with a storing energy of 100 kJ. The inner diameter of the coil is 10 mm and a peak field of 150 T can be obtained. The copper coil system was contained inside a large steel box to protect the optical apparatus and to shield the detector from any noise generated by the ex-

plosion of the coil. The sample is set in a small, hand-made cryostat which is set at the center of the single-turn coil. The copper coil is fixed between two electrodes in a large steel box, and the large current discharge explodes the coil violently. Because the explosion of the coil is directed in an outward direction, the cryostat and sample survive many such experiments. The field strength is determined by measuring the induced voltage in a calibrated pickup coil wound around the sample. A heater wire was also wound around the sample, and the experimental temperature was controlled between room temperature and about 600 K.

A water-cooled H₂O/D₂O vapor pulse laser was used to generate several lines in the far infrared with wavelengths ranging from 17 to 119 μ m. The radiation from the H₂O laser at 119 μ m is circularly polarized as described in Sec. III. The output beam from the laser was steered by some mirror optics and focused onto the sample at normal incidence. The transmitted radiation was detected with an extrinsic photoconductive detector (either Ga:Ge or Cu:Ge) which was cooled down to the helium temperature in a cryostat mounted in an electrically shielded box. The outputs of the detector were amplified by a high-frequency electronic circuit, and then fed by an optical fiber into one channel of a two-channel fast-response 2048-word digital recorder. The other recorder channel was used to monitor the magnetic-field signal from the pickup coil. With a system such as described above, it is possible to observe far-infrared cyclotron resonance up to 150 T with a very good signal-to-noise ratio.

III. RESULTS

A. Linear polarization

Figure 1 shows cyclotron-resonance (CR) absorption traces as a function of magnetic field, obtained for sample 1 at and above room temperature with 119- μ m radiation from an H₂O vapor laser and with magnetic field in the $\langle 110 \rangle$ crystallographic direction. The radiation beam was polarized by a linear polarizer. A large, broad peak, consisting of two lines at about 30 and 65–70 T, is observed. They increased in intensity with increasing temperature and disappeared at low temperatures below 0°C because of the carrier freeze-out. This suggests that these resonant absorption lines are due to cyclotron resonance of thermally excited free holes.

From the observed spectra shown in Fig. 1, we may say

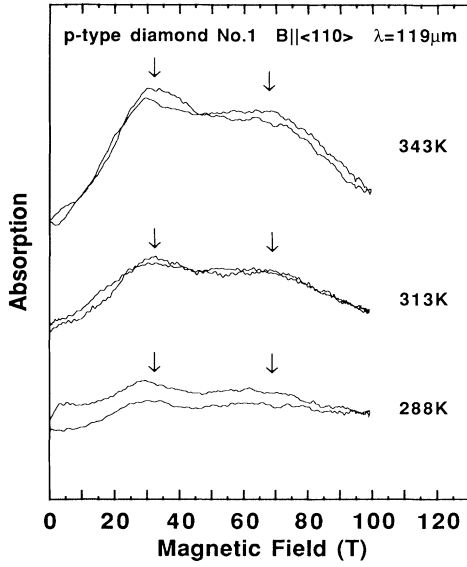


FIG. 1. Absorption spectra as a function of the magnetic field, obtained at several temperatures above room temperature for type-IIb diamond with the magnetic field oriented in the $\langle 110 \rangle$ crystallographic direction at 119- μm wavelength.

that a classical interpretation is valid because there does not seem to be any significant contribution from quantum effects. A curve-fitting procedure was adopted to obtain more accurate effective masses and scattering times. As is well known,¹⁴ the power absorbed by k th type of carriers in a magnetic field from a linearly polarized electromagnetic wave is proportional to

$$P_k = \sigma_k \left[\frac{1}{(\omega - \omega_{ck})^2 \tau^2 + 1} + \frac{1}{(\omega + \omega_{ck})^2 \tau^2 + 1} \right], \quad (1)$$

where σ_k is the dc conductivity for the k th carrier. Thus adding the absorptions for the two types of carriers with adjustable parameters $m^*(1)$, $m^*(2)$, $\tau(1)$, $\tau(2)$, and σ_1/σ_2 , we obtained $m^*(1) = (0.33 \pm 0.03)m_0$, $m^*(2) = (0.75 \pm 0.05)m_0$, $\omega\tau(1) = 2.2$, and $\omega\tau(2) = 1.5$ at 40°C. It may be worth pointing out here that this order of $\omega\tau$ was typical in the present experiments due to its low carrier mobility, and the observation of CR was made possible only by the use of extremely strong magnetic fields. In order to obtain the longest possible scattering time τ , the experimental temperature must be as low as possible. At these temperatures, however, carriers are frozen out because of the large binding energies of donors and acceptors. This is the dilemma which frequently arises in the case of large-gap semiconductors.

B. Photon energy dependence: band parabolicity

The cyclotron-resonance absorption traces for $\mathbf{B} \parallel \langle 110 \rangle$ at a wavelength of 28 μm are displayed in Fig. 2. The line $m^*(1)$ is again observed at 125 T with the same value of effective mass: $0.33m_0$. The first point to note is that the freeze-out temperature was very high compared to that at 119 μm . In fact, we could not see the resonances at room temperature at this wavelength.

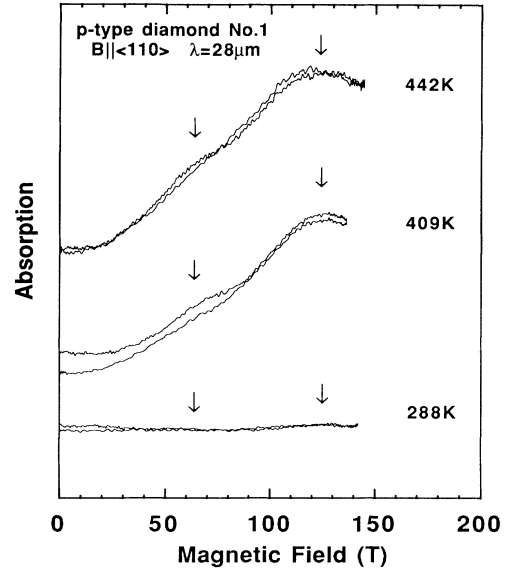


FIG. 2. Cyclotron-resonance absorption traces at 119, 36, and 28 μm at various temperatures obtained for sample 1. The magnetic field was oriented in the $\langle 110 \rangle$ direction.

This can be explained by assuming that only the $m^*(2)$ band, the resonance position of which is far above 150 T, is populated at room temperature because the energy difference between the edges of the two bands should be very large in such high magnetic fields. Another feature is the structure, peaking at about $0.13m_0$, observed in the lower-side shoulder of the $m^*(1)$ peak. From the temperature (35–40 meV) and the photon energy (44.2 meV), i.e., $\hbar\omega_c \approx kT$, it is possible that this structure is a quantum line. This structure was also observed at 36 μm together with the $m^*(1)$ line having the same value of mass.

Since the spin-orbit splitting in the valence band is very small in diamond (5–7 meV), the interaction between Γ_8 and Γ_7 bands is expected to be very strong. As a result, a large nonparabolicity is expected for all the three valence bands. However, as shown above, the $m^*(1)$ line was found to have almost the same value of effective mass throughout the entire energy range of the present experiment, i.e., 10.4–44.2 meV. The reason for this discrepancy is that $\hbar\omega_c > \Delta$, i.e., the energy range of our measurements, is far away from the highly nonparabolic region which is expected to be 0–6 meV. The experiments at $\hbar\omega_c < \Delta$ would be more interesting in this sense, but then the condition $\omega_c \tau > 1$ becomes impossible.

C. Circular polarization: electronlike transition

Next we present the experimental results with circularly polarized 119- μm laser radiations. A cyclotron-resonance peak obtained with a circularly polarized electromagnetic wave is in general more pronounced than with a linearly polarized wave even when the value of $\omega_c \tau$ is the same, since one can separate the active and inactive parts of a CR spectrum. In this respect, the use of circular polarization is particularly suitable for the measure-

ments of broad CR lines in low mobility semiconductors such as diamond. It is known that the $119\text{-}\mu\text{m}$ laser radiation from an H_2O laser is circularly polarized, but the sense of rotation is bistable.²⁸ In order to determine the absolute direction of the circular rotation and to determine the sign of the carriers in diamond, the cyclotron resonance of n -type GaAs was measured simultaneously with diamond.

Figures 3 and 4 show some typical transmission traces of circularly polarized radiations together with a magnetic-field trace as a function of time. For hole-cyclotron-resonance active (CRA) radiations, which correspond to time regions where the magnetic field is positive in Fig. 3 and negative in Fig. 4, a large absorption is observed for all three orientations as shown. The important point to note is that anisotropic behavior is observed in the hole-cyclotron-resonance inactive (CRI) part of the spectrum, namely in time regions where the magnetic field is negative in Fig. 3 and positive in Fig. 4. A small absorption peak or structure is observed in the background of a typical inactive CR spectrum. In particular, with the magnetic field in the $\langle 100 \rangle$ orientation, a prominent sharp absorption peak is observed for the hole-CRI polarization (this is of course CRA for electrons).

Figures 5 and 6 show the transmission spectra for magnetic fields in the $\langle 100 \rangle$ direction for the two senses of circular polarization at wavelength of $119\text{ }\mu\text{m}$ at various temperatures. For hole-CRA polarization, a broad, unresolvable peak which probably consists of two peaks is observed as shown in Fig. 5. For hole-CRI polarization, on the other hand, a well-defined, narrower absorption

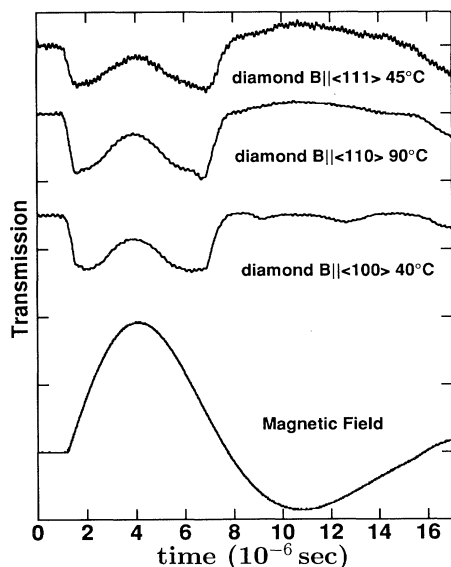


FIG. 3. Transmission traces of circularly polarized $119\text{-}\mu\text{m}$ radiation through semiconducting diamond as a function of time. The magnetic-field trace is also indicated. The field is applied in the $\langle 100 \rangle$, $\langle 111 \rangle$, and $\langle 110 \rangle$ crystallographic directions. The transmission trace in the region where the magnetic field is positive corresponds to CRA, and the trace where the field is negative corresponds to CRI.

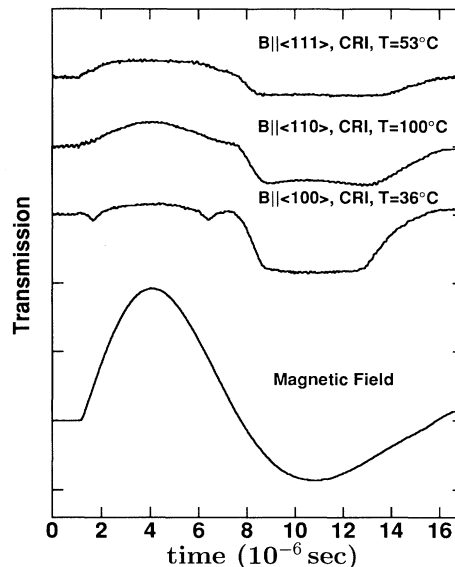


FIG. 4. Transmission traces of circularly polarized $119\text{-}\mu\text{m}$ radiation through semiconducting diamond as a function of time. The magnetic-field trace is also indicated. The field is applied in the $\langle 100 \rangle$, $\langle 111 \rangle$, and $\langle 110 \rangle$ crystallographic directions. The transmission trace in the region where the magnetic field is positive corresponds to CRI, and the trace where the field is negative corresponds to CRA.

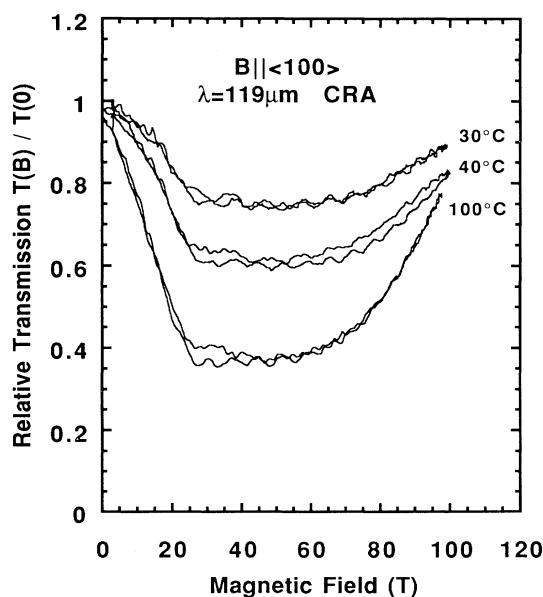


FIG. 5. Magnetic-field dependence of the transmission of $119\text{-}\mu\text{m}$ laser radiation through semiconducting diamond for the hole-CRA sense of circular polarization at various temperatures. The field is applied in the $\langle 100 \rangle$ crystallographic direction. A broad absorption peak, consisting of two lines, is observed to increase in intensity with increasing temperature.

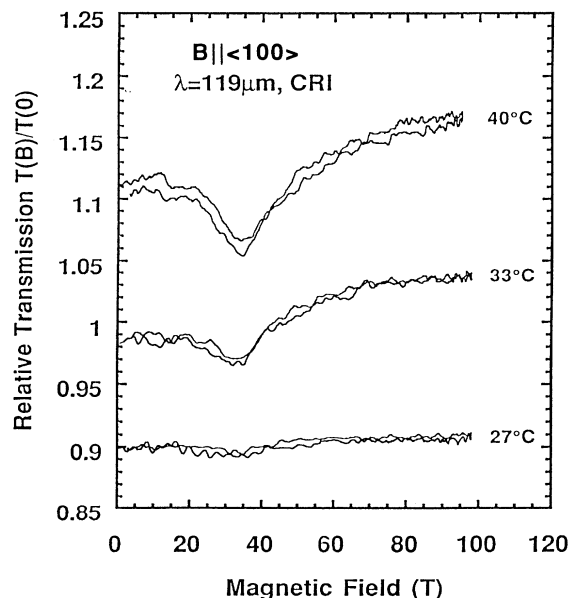


FIG. 6. Magnetic-field dependence of the transmission of 119- μm laser radiation through semiconducting diamond for the hole-CRI sense of circular polarization at various temperatures. The field is applied in the $\langle 100 \rangle$ crystallographic direction. A well-defined prominent absorption peak is observed at 33 T. From temperature dependence it can be said that this peak is due to cyclotron resonance of a free carrier, which has an *electronlike* cyclotron orbit.

peak is observed at 33 T as shown in Fig. 6. All these peaks are evidently due to cyclotron resonance of thermally excited free carriers since they increase in intensity with increasing temperature. The prominent peak observed for CRI suggests that there is one type of carrier which has an *electronlike* cyclotron orbit.

Figure 7 displays absorption spectrum at 100°C for the two senses of circular polarization. This data were obtained during a single shot, i.e., they were obtained while the field was swept between -40 and 100 T in order of μs . A curve-fitting procedure was again adopted as in Sec. III A above. In this case, the expression for a circular polarization

$$P_k = \sigma_k \frac{1}{(\omega - \omega_{ck})^2 \tau^2 + 1} \quad (2)$$

was employed instead of Eq. (1). Furthermore, three types of carriers were assumed to exist rather than two. In Fig. 7, the solid line denotes the experimental trace, the three broken lines denote theoretical curves, and the sum of the three theoretical curves are indicated as a dotted line which is almost identical with the experimental trace. This figure tells us that the experimental trace can be well explained by the sum of three theoretical traces, assuming that there are three types of carriers and one of them has an *electronlike* orbit. The three cyclotron masses thus determined for $\mathbf{B} \parallel \langle 100 \rangle$ are $m^*(1) = -0.38m_0$, $m^*(2) = +0.31m_0$, and $m^*(3) = +0.70m_0$, where “-” means “*electronlike*” and “+”

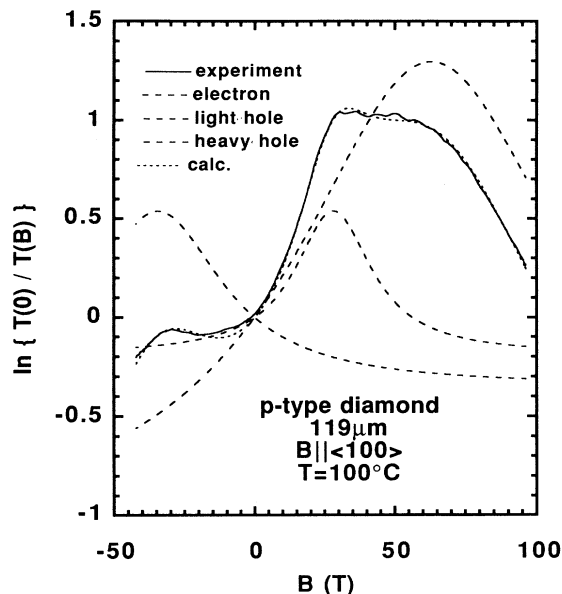


FIG. 7. Absorption spectrum at 100°C for the two senses of circular polarization and with the magnetic field oriented in the $\langle 100 \rangle$ direction. The solid line denotes the experimental trace, the three broken lines denote theoretical curves, and the sum of the three theoretical curves are indicated as a dotted line which is almost identical with the experimental trace.

means “*holelike*.” It is worthwhile to point out that although the apparent absorption intensity of the *electronlike* peak is small compared to the other two peaks, its actual intensity is comparable with the other two, as the theoretical curves in Fig 7 indicates. A large part of the intensity of the peak is lost or eliminated by the existence of the inactive part of the other two peaks, and the inverse is also true.

The curve fitting was also conducted on the traces obtained for $\mathbf{B} \parallel \langle 111 \rangle$ and $\langle 110 \rangle$ as shown in Figs. 8 and 9. In these cases, however, the peak in the CRI spectrum is dull or vague compared to the case of $\mathbf{B} \parallel \langle 100 \rangle$, and the deviation of the theoretical curve from the experimental curve in the CRI part is larger. Nonetheless, a certain structure definitely exists in the CRI spectrum, and the excellent fit in the CRA spectrum assures us that the model is correct. Figure 10 summarizes the cyclotron masses obtained from the line-shape analysis, where masses are expressed in units of m_0 (free-electron mass), and the angle between the field direction and the $\langle 100 \rangle$ direction in a (110) plane is taken as the abscissa.

The existence of the *electronlike* orbit admits three different interpretations. One explanation may be that there are “*real*” electrons in our samples. If this is the case, the transverse effective mass $m_t^* = 0.38m_0$ may be concluded from the experimental results for $\mathbf{B} \parallel \langle 100 \rangle$, based on the theoretical prediction that the conduction band minima lie in the X direction. However, this possibility is not likely since effective donors have never been discovered for diamond. The second possibility is that some of the transitions between low Landau indices may be allowed for CRI polarizations. However, since the

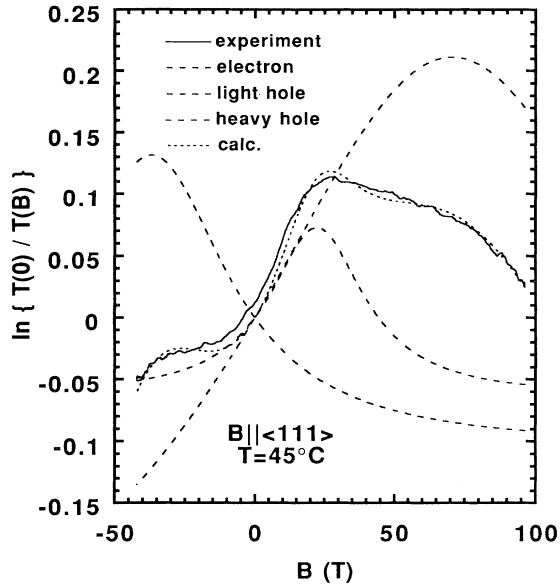


FIG. 8. Absorption spectrum at 45°C for the two senses of circular polarization and with the magnetic field oriented in the $\langle 111 \rangle$ direction. The solid line denotes the experimental trace, the three broken lines denote theoretical curves, and the sum of the three theoretical curves is indicated by a dotted line.

resonance peak was observed in a wide range of temperature above the photon energy (10.4 meV), it is not likely that this line is due to quantum cyclotron resonance. Another, more plausible explanation is that the effective masses of heavy and/or light holes are negative (electron-like) in some direction(s). As Eremets has also pointed

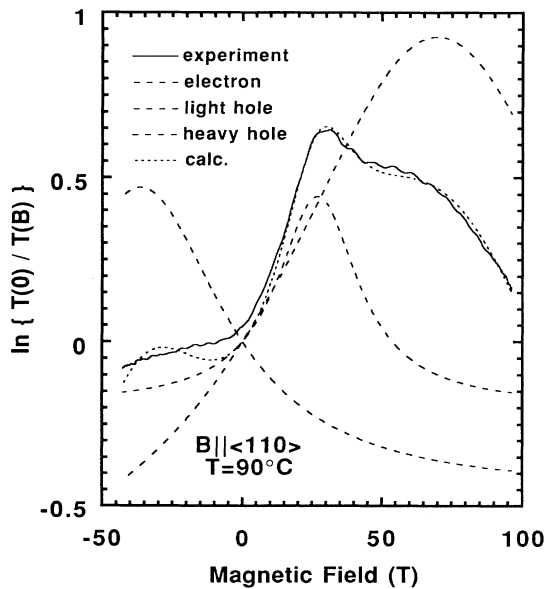


FIG. 9. Absorption spectrum at 90°C for the two senses of circular polarization and with magnetic field oriented in the $\langle 110 \rangle$ direction. The solid line denotes the experimental trace, the three broken lines denote theoretical curves, and the sum of the three theoretical curves is indicated by a dotted line.

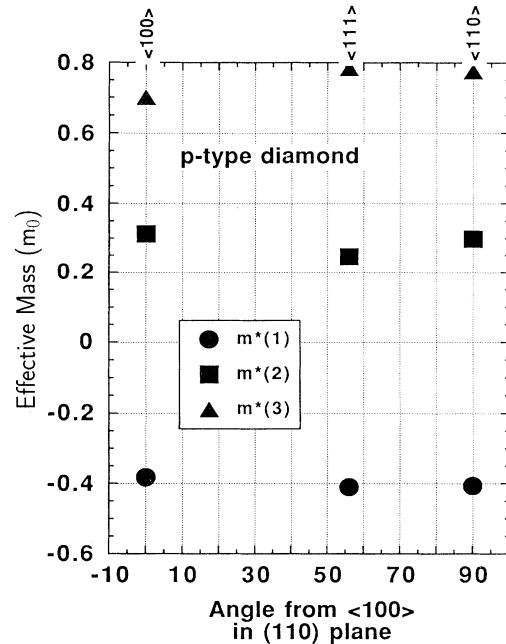


FIG. 10. The obtained cyclotron masses in diamond at 119- μm wavelength for magnetic-field directions in a (110) plane. Masses are expressed in units of m_0 , and the angle between the field and the $\langle 100 \rangle$ direction is taken as the abscissa.

out,²¹ there is a possibility that light and heavy holes may have negative slopes in the energy dispersion curves if a certain combination of γ parameters are chosen.

D. Millimeter-wave experiments

The experimental results described in the preceding sections are considerably different from the millimeter-wave CR discussed by Rauch 30 years ago,^{9,10} although it is true that the experimental temperature and the photon energy range are also very different. Our results were obtained at high temperatures on thermally excited free holes. Though the scattering time τ was small, $\omega_c \tau$ became larger than unity by the use of ultrahigh magnetic fields. Rauch's results, on the other hand, were obtained at liquid-helium temperatures, 1.2–4 K, on optically excited free holes. In Rauch's experiments, the quantum condition was obviously satisfied so that interpretation is more difficult than in our case, although he used classical interpretation. In any way, Rauch's work has long been the single report on the direct determination of the effective-mass parameters for diamond.

In order to check Rauch's results in the millimeter-wave range, magneto transmission experiments were also performed at 156 GHz over a wide range of temperature in pulsed magnetic fields up to 20 T with a duration of order of ms, produced by a nondestructive method. Three resonance peaks have been observed as shown in Fig. 11, having effective masses $m^*(1)=0.92m_0$, $m^*(2)=1.26m_0$, and $m^*(3)=1.98m_0$, which are close to but slightly different from Rauch's values. However, these peaks were not the cyclotron-resonance absorptions but

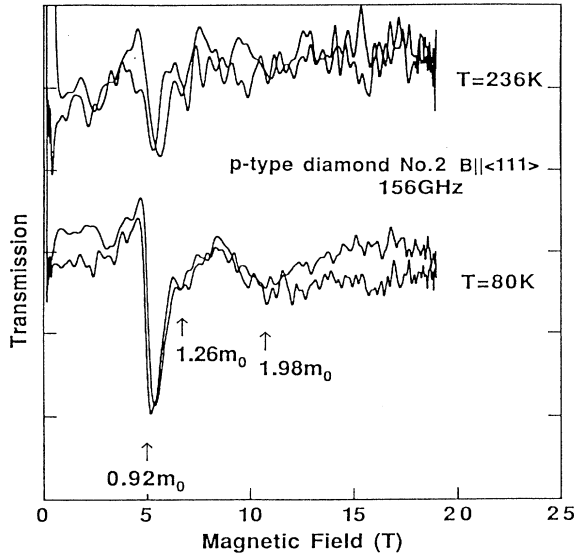


FIG. 11. Millimeter wave magnetotransmission spectra of semiconducting diamond at 156 GHz in pulsed magnetic fields up to 20 T.

were probably due to the impurity transitions, since they gained their intensity with lowering temperature.

The possibility still remains that the absorption lines observed by Rauch are due to the quantum cyclotron resonance of optically excited free holes, since he used an external modulating light. If that is the case, a much more detailed and accurate model is required to understand the data. Nonetheless, it seems most likely that Rauch observed the same peaks as our present experiment at 156 GHz.

IV. DISCUSSION

Based on the results of cyclotron resonance described in Sec. III, let us now consider the valence-band structure in diamond. In the following, we develop an approximation method which seems to be most suitable for the determination of the γ parameters of diamond from our experimental results obtained at high fields and at high temperatures. As a consequence of the consideration, we will show that higher-order terms are necessary in order to describe correctly the structure of the valence band in diamond.

Since the present experiments were mostly performed at higher temperatures than the cyclotron energy, i.e., $\hbar\omega_c < kT$, we may say that the absorption lines observed are the transitions between adjacent Landau levels bearing high quantum numbers with an almost equal spacing (the classical limit.) To deduce the γ parameters^{15,29} from the experimental results, the six-dimensional effective-mass Hamiltonian for the degenerate valence band is considered. In the usual way of the effective-mass approximation for the valence band in Ge and Si, the six-dimensional space splits into a four-dimensional $J = \frac{3}{2}$ subspace (Γ_8) and a two-dimensional $J = \frac{1}{2}$ subspace (Γ_2), and it is sufficient to take into account only the

four-dimensional subspace in order to analyze cyclotron resonance data so long as the condition $\hbar\omega_c < \Delta$ holds. However, in our case of ultrahigh-field far-infrared measurements, $\hbar\omega_c = 10\text{--}45$ meV and $\Delta = 6$ meV, therefore the four-dimensional picture is completely inappropriate. Hence classical approximations and relations such as

$$m/m_{lh}, m/m_{hh} = \gamma_1 \pm [\gamma'^2 + 3\gamma''^2]^{1/2},$$

$$\epsilon_{lh}(\mathbf{k}), \epsilon_{hh}(\mathbf{k}) = Ak^2 \pm [B^2k^4 + C^2(k_x^2k_y^2 + k_y^2k_z^2 + k_z^2k_x^2)]^{1/2}, \quad (3)$$

$$\epsilon_{so}(\mathbf{k}) = -\Delta + Ak^2$$

cannot be used to analyze our data. In order to treat accurately the interaction between the Γ_8 and Γ_7 bands, we have to deal with the full 6×6 effective-mass Hamiltonian matrix.

We start with the following form of the effective-mass Hamiltonian matrix for the valence band in diamond:

$$D = \begin{pmatrix} D_a & D_c \\ D_c^* & D_b \end{pmatrix}, \quad (4)$$

where D_a , D_b , and D_c are 3×3 matrices whose components are given by setting $P=0$ in the 4×4 Pidgeon-Brown Hamiltonian matrices,³⁰ since the interaction between conduction and valence bands is unimportant in large-gap materials. We confine ourselves to the case where $n = \infty$ and $\Delta = 0$, which seem to be reasonable approximations for the case of classical cyclotron resonance in diamond. Also, we neglect the off-diagonal term D_c assuming it is small. Under these assumptions, the secular equations of the 3×3 Hamiltonian matrices D_a and D_b reduce to

$$\begin{vmatrix} (A+B)+\alpha & \sqrt{3}C & -\sqrt{6}iB \\ \sqrt{3}C & (A-B)+\alpha & -\sqrt{2}iB \\ \sqrt{6}iB & \sqrt{2}iB & A+\alpha \end{vmatrix} = 0, \quad (5)$$

where $\alpha = -m_0/m^*$ is defined as the dimensionless energy, and

$$\begin{aligned} A &= \gamma_1, \\ B &= \gamma' = \gamma_3 + (\gamma_2 - \gamma_3)[(3 \cos^2\theta - 1)/2]^2, \\ C &= \gamma'' = \frac{2}{3}\gamma_3 + \frac{1}{3}\gamma_2 + \frac{1}{6}(\gamma_2 - \gamma_3)[(3 \cos^2\theta - 1)/2]^2. \end{aligned} \quad (6)$$

The sign of m^* is taken to be positive when it is holelike. From Eqs. (5) and (6), we obtain a cubic equation in α :

$$\alpha^3 + u\alpha^2 + v\alpha + w = 0, \quad (7)$$

where u, v, w are simple functions of A, B, C . For a fixed θ , Eq. (7) has three solutions, $\alpha_i (i = 1, 2, 3)$, corresponding to the three valence bands, and the coefficients u, v, w are related to them by

$$\begin{aligned} u &= -(\alpha_1 + \alpha_2 + \alpha_3), \\ v &= \alpha_1\alpha_2 + \alpha_2\alpha_3 + \alpha_3\alpha_1, \\ w &= -\alpha_1\alpha_2\alpha_3. \end{aligned} \quad (8)$$

Then it can be easily obtained that

$$\gamma_1 = -\frac{1}{3}(\alpha_1 + \alpha_2 + \alpha_3) = \frac{m_0}{3} \left[\frac{1}{m_1^*} + \frac{1}{m_2^*} + \frac{1}{m_3^*} \right], \quad (9)$$

meaning that γ_1 is the average of the three inverse cyclotron masses observed with the magnetic field fixed in an arbitrary crystallographic direction. Furthermore, γ_2 and γ_3 are obtained from simple coupled numerical equations with inputs of experimental results α_i ($i=1,2,3$).

In the following, let us assume that $m^*(1)$, $m^*(2)$, and $m^*(3)$ correspond to heavy, light, and split-off holes, respectively. The most reliable experimental data for $\mathbf{B} \parallel \langle 100 \rangle$, i.e., $\alpha_1 = +2.61$, $\alpha_2 = -3.20$, and $\alpha_3 = -1.43$, were employed as input parameters to the coupled equation, and two sets of γ parameters, $(\gamma_1, \gamma_2, \gamma_3, \kappa) = \text{no. 1}(0.67, -0.57, -2.23, -3.50)$, no. 2(0.67, -0.98, 0.56, -0.98), were obtained as solutions. Here, the relation between the parameters¹⁵

$$\kappa = -\frac{1}{3}\gamma_1 + \frac{2}{3}\gamma_2 + \gamma_3 - \frac{2}{3} \quad (10)$$

was used to estimate κ . These sets were then substituted into the secular equation with finite n and $\Delta = 6$ meV to calculate the Landau levels and to see if the observed absorption peaks can be interpreted as transitions between equally spaced Landau levels bearing high quantum numbers. As expected from the fact that we started with the experimental data with magnetic field in the $\langle 100 \rangle$ direction, both of the sets were found to give Landau levels which are consistent with the experimental results for $\mathbf{B} \parallel \langle 100 \rangle$. For $\mathbf{B} \parallel \langle 110 \rangle$ and $\mathbf{B} \parallel \langle 111 \rangle$, however, the calculation could not explain any of the observed lines.

To understand the origin of the discrepancy between experiment and calculation, let us next consider the band dispersion curves of the three holes with the new parameters using the second-order $\mathbf{k} \cdot \mathbf{p}$ perturbation theory for the degenerate valence bands in Ge and Si developed by Kane.³¹ As already shown in Kane's original paper,³¹ the two Γ_8 bands bend upward and the Γ_7 band bends downward with increasing $|\mathbf{k}|$ for all three symmetric directions, as a result of the interaction between them. Consequently, the inequality of the three effective masses at the band edge, namely $m_{\text{hh}}^* > m_{\text{so}}^* > m_{\text{lh}}^*$, is no longer correct at higher energies. As one deviates from the band edge, m_{hh}^* and m_{lh}^* increase, and m_{so}^* decreases, and finally m_{lh}^* exceeds m_{so}^* at a certain energy. This characteristic energy is, of course, of the order of the spin-orbit splitting Δ . Owing to the relatively large Δ in Ge (290 meV) and Si (44 meV), this energy is far above usual temperature range of transport experiments. In addition, the cyclotron resonance of the split-off hole has never been observed in Ge and Si. Thus this " $m_{\text{lh}}^* - m_{\text{so}}^*$ crossing" has not yet been checked. This effect can also be found for the constant energy surfaces (cyclotron orbits) of the holes in Ge and Si in our calculation. Because of the nonparabolicity resulting from the interaction, the shape of the energy contour changes dramatically at the characteristic energy. This is known as the " $\langle 110 \rangle$ swelling" and has been experimentally observed as a change in the anisotropy of the galvanomagnetic effects in p -type Si.³²

As already stated, the spin-orbit splitting (i.e., the energy difference between Γ_8 and Γ_7) is extremely small in di-

amond compared to Ge and Si. Because of that, one can expect the strong Γ_8 - Γ_7 repulsion as well as the participation of the split-off hole in electrical conduction. Substituting our parameters and $\Delta = 6$ meV into Kane's formula gave some completely conduction-band-like dispersion curves for valence bands in some directions, i.e., the energy-band function $\epsilon(\mathbf{k})$ increased monotonously with $|\mathbf{k}|$ and never bent downward. The negative effective mass is not surprising if we think of the large fundamental energy gap and the small spin-orbit splitting in diamond, both of which make m_{hh}^* and m_{lh}^* very large and even negative. However, the conduction-band-like valence bands should be possible only in the vicinity of the top of the valence-band, and they must bend downward again somewhere in the high-energy range. This would introduce additional cyclotron orbits (e.g., volcano type) that we have not taken into consideration, and the existence of these orbits would explain why the calculated Landau levels did not agree with experiments. To describe these orbits, the second-order Hamiltonian is insufficient, and k^4 terms are necessary in the Hamiltonian. However, the inclusion of the k^4 terms in the Hamiltonian necessitates the inclusion of a large number of extra band parameters in the theory. Suzuki and Hensel³³ constructed the most general k^4 Hamiltonian for the Γ_8 band by purely group-theoretical means. The Hamiltonian they obtained contains seven independent parameters in addition to the usual three constants, even in the spherical approximation. Therefore, the most general k^4 Hamiltonian to describe all the three valence bands would have even more parameters, and it would be almost impossible to determine all the parameters by the classical cyclotron-resonance experiments. Further complication would come from the " k_H effect," which we have neglected so far but which should have significant effects especially in the case of complicated bands. Finally, it should be noted that the magnetic breakthrough should be also possible since $\hbar\omega_c > \Delta$. If this is the case, the orbits of the three bands mix and the interpretation above does not make sense anymore.

In summary, we made an observation of the cyclotron resonance of thermally excited free holes in diamond by using pulsed ultrahigh magnetic fields up to 150 T. Three different peaks of cyclotron resonance were observed corresponding to the three holes in the valence band. By the use of circularly polarized radiations, we showed that there is one electronlike cyclotron orbit in the valence band in our experimental energy range. Starting from the 6×6 effective Hamiltonian matrix in the classical limit with an approximation of $\Delta = 0$, two possible sets of γ parameters were deduced. Both Landau levels and band dispersion curves were calculated with the parameters, and it was found that higher-order terms must be taken into account to explain all the experimental data. Therefore, the important conclusion of the present work is that the valence band in diamond is much more complicated than that in Ge and Si, because of the strong Γ_8 - Γ_7 interaction resulting from the very small spin-orbit splitting, which was experimentally evidenced by the application of extremely strong magnetic fields.

To clarify the detailed valence-band structure in the

neighborhood of the Γ point more accurately, the following experiments would be useful.

(a) First, diamond specimens with higher carrier mobility are necessary in order to get narrower absorption peaks.

(b) Cyclotron-resonance experiments at a lower photon energy range, 0–6 meV, would clarify the detailed nonparabolicity of the valence bands, because nonparabolicity is expected to be very strong, in the energy range below Δ .

(c) The application of uniaxial stresses to the crystal

would be useful, because it removes the degeneracy at $\mathbf{k} = \mathbf{0}$ and simplifies the interpretation of the spectra. The decoupled bands should have ellipsoidal energy surfaces like the conduction bands.

ACKNOWLEDGMENT

The authors are indebted to Professor K. Suzuki of Tokyo Metropolitan Institute of Technology for stimulating discussions.

*Present address: State University of New York at Buffalo, Buffalo, NY 14260.

†Present address: Himeji Institute of Technology, Harima, Hyogo 678-12, Japan.

¹J. F. H. Custers, *Physica* **18**, 489 (1952); *ibid.* **20**, 183 (1954).

²For the review of the electrical properties of type-IIb diamond, see, for example, A. T. Collins and E. C. Lightowers, in *The Properties of Diamond*, edited by J. E. Field (Academic, London, 1979), pp. 79–105; V. K. Bashenov, I. M. Vikulin, and A. G. Gontar, *Fiz. Tekh. Polopruvodn.* **19**, 1345 (1985) [*Sov. Phys. Semicond.* **19**, 829 (1985)]; see also Ref. 21.

³J. J. Brophy, *Phys. Rev.* **99**, 82, 1336 (1955).

⁴I. G. Austin and R. Wolfe, *Proc. Phys. Soc. B* **69**, 329 (1956).

⁵P. T. Wedepohl, *Proc. Phys. Soc. B* **70**, 177 (1957).

⁶P. J. Dean, E. C. Lightowers, and D. R. Wright, *Phys. Rev.* **140**, A352 (1965).

⁷W. Salsow, T. K. Bergstresser, and M. L. Cohen, *Phys. Rev. Lett.* **16**, 354 (1966).

⁸F. Herman, C. D. Kuglin, K. F. Cuff, and R. L. Kortum, *Phys. Rev. Lett.* **11**, 541 (1963).

⁹C. J. Rauch, *Phys. Rev. Lett.* **7**, 83 (1961).

¹⁰C. J. Rauch, in *Proceedings of the International Conference on the Physics of Semiconductors*, Exeter, edited by A. C. Stickland (The Institute of Physics and the Physical Society, London, 1962), p. 276.

¹¹V. Prosser, *Czech. J. Phys.* **B15**, 128 (1964).

¹²E. W. J. Mitchell, in *Proceedings of the International Symposium on Diamond, Paris, 1962*, edited by Patric Greene (Industrial Diamond Information Bureau, London, 1963), pp. 241–251.

¹³D. M. S. Bagguley, G. Vella-Coleiro, S. D. Smith, and C. J. Summers, *J. Phys. Soc. Jpn.* **21**, 244 (1966).

¹⁴G. Dresselhaus, A. F. Kip, and C. Kittel, *Phys. Rev.* **98**, 368 (1955).

¹⁵P. Lawaetz, *Phys. Rev. B* **4**, 3460 (1970).

¹⁶L. Reggiani, S. Bosi, C. Canali, F. Nava, and S. F. Kozlov,

Solid State Commun. **30**, 333 (1979).

¹⁷F. Nava, C. Canali, J. Jacoboni, L. Reggiani, and S. F. Kozlov, *Solid State Commun.* **33**, 475 (1980).

¹⁸L. Reggiani, S. Bosi, C. Canali, F. Nava, and S. F. Kozlov, *Phys. Rev. B* **23**, 3050 (1981).

¹⁹V. K. Bashenov, A. G. Gontar, and A. G. Petukhov, *Phys. Status Solidi B* **108**, K139 (1981).

²⁰V. V. Struzhkin and M. I. Eremets, *Fiz. Tekh. Polopruvodn.* **22**, 1488 (1988) [*Sov. Phys. Semicond.* **22**, 943 (1988)].

²¹M. I. Eremets, *Semicond. Sci. Technol.* **6**, 439 (1991).

²²K. Nakao, F. Herlach, T. Goto, S. Takeyama, T. Sakakibara, and N. Miura, *J. Phys. E* **18**, 1018 (1985).

²³S. Takeyama, K. Amaya, T. Nakayama, M. Ishizuka, K. Nakao, T. Sakakibara, T. Goto, N. Miura, Y. Ajiro, and H. Kikuchi, *J. Phys. E* **21**, 1025 (1988).

²⁴N. Miura, in *Physical Phenomena at High Magnetic Fields*, edited by E. Manousakis, P. Schlottmann, P. Kumar, K. Bedell, and F. M. Mueller (Addison-Wesley, New York, 1992), pp. 589–603.

²⁵J. Kono, N. Miura, S. Takeyama, H. Yokoi, N. Fujimori, Y. Nishibayashi, T. Nakajima, K. Tsuji, and M. Yamanaka, *Physica B* **184**, 178 (1993).

²⁶J. Kono, S. Takeyama, H. Yokoi, N. Miura, M. Yamanaka, M. Shinohara, and K. Ikoma, preceding paper, *Phys. Rev. B* **48**, 10909 (1993).

²⁷N. Miura, H. Yokoi, J. Kono, and S. Sasaki, *Solid State Commun.* **79**, 1039 (1991).

²⁸See, for example, G. W. Chantry, *Submillimeter Spectroscopy* (Academic, New York, 1971), Chap. 6, p. 268.

²⁹J. M. Luttinger, *Phys. Rev.* **102**, 1030 (1956).

³⁰C. R. Pidgeon and R. N. Brown, *Phys. Rev.* **146**, 575 (1966).

³¹E. O. Kane, *J. Phys. Chem. Solids* **1**, 82 (1956).

³²H. Miyazawa, K. Suzuki, and H. Maeda, *Phys. Rev.* **131**, 2442 (1963).

³³K. Suzuki and J. C. Hensel, *Phys. Rev. B* **9**, 4184 (1974).